Widely tunable single-photon source with high spectral-purity from telecom wavelength to mid-infrared wavelength based on MgO: PPLN

Chang-Wei Sun(孙昌伟), Yu Sun(孙宇), Jia-Chen Duan(端家晨), Guang-Tai Xue(薛广太), Yi-Chen Liu(刘奕辰), Liang-Liang Lu(陆亮亮), Qun-Yong Zhang(张群永), Yan-Xiao Gong(龚彦晓), Ping Xu(徐平), and Shi-Ning Zhu(祝世宁)

Citation: Chin. Phys. B, 2021, 30 (**10**): 100312. DOI: 10.1088/1674-1056/ac20cb
Journal homepage: http://cpb.iphy.ac.cn; http://iopscience.iop.org/cpb

What follows is a list of articles you may be interested in

Measurement-device-independent quantum dialogue

Guo-Fang Shi(石国芳)
Chin. Phys. B, 2021, 30 (**10**): 100303. DOI: 10.1088/1674-1056/ac140a

Discrete wavelet structure and discrete energy of classical plane light waves

Xing-Chu Zhang(张兴初) and Wei-Long She(佘卫龙)
Chin. Phys. B, 2021, 30 (**4**): 040301. DOI: 10.1088/1674-1056/abcf34

Performance optimization for quantum key distribution in lossy channel using entangled photons

Yu Yang(杨玉), Luping Xu(许录平), Bo Yan(阎博), Hongyang Zhang(张洪阳), Yanghe Shen(申洋赫)
Chin. Phys. B, 2017, 26 (**11**): 110305. DOI: 10.1088/1674-1056/26/11/110305

Efficient entanglement concentration for arbitrary less-entangled NOON state assisted by single photons

Lan Zhou(周澜) and Yu-Bo Sheng(盛宇波)
Chin. Phys. B, 2016, 25 (**2**): 020308. DOI: 10.1088/1674-1056/25/2/020308

Optimal entanglement concentration for three-photon W states with parity check measurement

Zhou Lan, Sheng Yu-Bo, Zhao Sheng-Mei
Chin. Phys. B, 2013, 22 (**2**): 020307. DOI: 10.1088/1674-1056/22/2/020307

RAPID COMMUNICATION

Widely tunable single-photon source with high spectral-purity from telecom wavelength to mid-infrared wavelength based on MgO:PPLN*

Chang-Wei Sun(孙昌伟)[1], Yu Sun(孙宇)[1], Jia-Chen Duan(端家晨)[1], Guang-Tai Xue(薛广太)[1], Yi-Chen Liu(刘奕辰)[1], Liang-Liang Lu(陆亮亮)[1,2], Qun-Yong Zhang(张群永)[3], Yan-Xiao Gong(龚彦晓)[1], Ping Xu(徐平)[1,†], and Shi-Ning Zhu(祝世宁)[1]

[1] *National Laboratory of Solid State Microstructures and School of Physics, Nanjing University, Nanjing* 210093, *China*
[2] *Key Laboratory of Optoelectronic Technology of Jiangsu Province, School of Physical Science and Technology, Nanjing Normal University, Nanjing* 210023, *China*
[3] *Faculty of Mathematics and Physics, Huaiyin Institute of Technology, Huaian* 223003, *China*

(Received 10 August 2021; revised manuscript received 18 August 2021; accepted manuscript online 25 August 2021)

By utilizing the extended phase-matching (EPM) method, we investigate the generation of single photons with high spectral-purity in a magnesium-doped periodically-poled lithium niobate (MgO:PPLN) crystal via the spontaneous parametric down-conversion (SPDC) process. By adjusting the temperature and pump wavelength, the wavelength of the single photons can be tuned from telecom to mid-infrared (MIR) wavelengths, for which the spectral-purity can be above 0.95 with high transmission filters. In experiments, we engineer a MgO:PPLN with poling period of 20.35 μm which emits the EPM photon pair centered at 1496.6 nm and 1644.0 nm and carry out the joint spectral intensity (JSI) and Glauber's second-order self-correlation measurements to characterize the spectral purity. The results are in good agreement with the numerical simulations. Our work may provide a valuable approach for the generation of spectrally pure single photons at a wide range of wavelengths which is competent for various photonic quantum technologies.

Keywords: single photons, quantum technologies, periodically-poled lithium niobate

PACS: 03.67.–a, 03.67.Hk, 42.50.Ex, 42.65.–k **DOI:** 10.1088/1674-1056/ac20cb

1. Introduction

The heralded single-photon sources with high spectral-purity are key for the applications of quantum information processing (QIP) including quantum computing,[1–4] boson sampling,[5–8] and quantum repeaters[9,10] for long-distance quantum communication due to the requirements of high-visibility interference between individual photons. Usually, much more attention has been paid on the telecommunication wavelengths.

In recent years, the single-photon sources in the mid-infrared (MIR) window have some other technological applications, such as quantum communication,[11] imaging[12,13] and gas sensing.[14,15] By improving the bandwidth and reducing the atmospheric scattering loss, the single-photon sources of MIR wavelength are in high demand for the long-distance quantum communication networks in free-space[16,17] and quantum lidar.[18,19]

Spontaneous parametric down-conversion (SPDC) and four-wave-mixing (SFWM) are commonly used to generate heralded single photons.[20–28] Due to the high second-order nonlinear susceptibility and flexible wavelength-tunable processes, the quasi-phase-matched (QPM) SPDC is extensively used in experiments.[27,29] Introducing the periodic ferroelectric domain inversion in nonlinear crystals, such as lithium niobate (LN), is an easy way to fulfill the QPM conditions. In SPDC processes, when the laws of energy conservation and momentum conservation are satisfied, a pump photon can probabilistically be converted into a pair of signal–idler photons. The conservations of the energy and momentum lead to a strong spectral correlation between the generated photon pairs which can be used to realize different quantum technologies.[30,31]

To improve the spectral-purity of photon pairs, i.e., make the two photons uncorrelated in frequency, a post-selecting method is popular where narrow bandpass filters are employed to reduce the spectral correlations.[32–34] However, this often comes at a cost of decreasing the generation rate and heralding efficiency, which are critical for some scaling applications, such as quantum computing[1–4] and boson sampling.[5–8]

To this end, the extended phase-matching (EPM)[35,36] emerges as a desirable way to balance the purity and efficiency. In this process, the group velocity matching (GVM) needs to be satisfied, and then, the poling period of the nonlinear crystal, pump laser, and QPM process should be selected properly.[24,37–40]

In this paper, by utilizing the EPM method, we show a

*Project supported by the National Basic Research Program of China (Grant Nos. 2017YFA0303700 and 2019YFA0308700) and the National Natural Science Foundation of China (Grant Nos. 11627810 and 11690031).

†Corresponding author. E-mail: pingxu520@nju.edu.cn

widely tunable non-degenerate single-photon source with high spectral-purity in a single MgO:PPLN with the doping ratio of 5 mol%. The wavelengths of the down-converted photons can be tuned from telecommunication band to mid-infrared band.

2. Theory

In a collinear SPDC process, the photon-pair state can be written as

$$|\Psi\rangle = A_0 \int_0^\infty \int_0^\infty \mathrm{d}\omega_\mathrm{s}\,\mathrm{d}\omega_\mathrm{i} f(\omega_\mathrm{s},\omega_\mathrm{i}) a_\mathrm{s}^\dagger(\omega_\mathrm{s}) a_\mathrm{i}^\dagger(\omega_\mathrm{i})|\mathrm{vac}\rangle, \quad (1)$$

where $|\mathrm{vac}\rangle$ represents the vacuum state, ω_s and ω_i are the angular frequencies, and subscripts s and i represent the signal and idler photons. $a_\mathrm{s}^\dagger$ and $a_\mathrm{i}^\dagger$ are the creation operators for the down-conversion photons. The coefficient A_0 absorbs all the constants and slowly varying functions of frequency. The joint spectral amplitude (JSA) demonstrates the spectral correlation between the signal and idler photons, which can be written as

$$f(\omega_\mathrm{s},\omega_\mathrm{i}) = \alpha(\omega_\mathrm{s}+\omega_\mathrm{i})\phi(\omega_\mathrm{s},\omega_\mathrm{i}), \quad (2)$$

where $\alpha(\omega_\mathrm{s}+\omega_\mathrm{i})$ is the pump envelope amplitude (PEA) and $\phi(\omega_\mathrm{s},\omega_\mathrm{i})$ is the phase matching amplitude (PMA). The PEA is a Gaussian distribution and the PMA equation can be written as

$$\phi(\omega_\mathrm{s},\omega_\mathrm{i}) = \mathrm{e}^{-\mathrm{i}\frac{\Delta kL}{2}}\mathrm{Sinc}\frac{\Delta kL}{2}, \quad (3)$$

where L is the length of the nonlinear crystal, Δk is the wavevectors mismatch between the pump and down-converted photons, which can be written as

$$\Delta k = k_\mathrm{p} - k_\mathrm{s} - k_\mathrm{i} - k_\mathrm{G}, \quad (4)$$

where $k_\mathrm{G} = 2\pi/\Lambda$ is the reciprocal wave with poling period Λ in the nonlinear crystal. The value of Λ is determined by

$$\Lambda = \frac{2\pi}{k_\mathrm{p}-k_\mathrm{s}-k_\mathrm{i}} = \frac{1}{\frac{n_\mathrm{p}}{\lambda_\mathrm{p}} - \frac{n_\mathrm{s}}{\lambda_\mathrm{s}} - \frac{n_\mathrm{i}}{\lambda_\mathrm{i}}}, \quad (5)$$

where n_j ($j = \mathrm{p,s,i}$) is the index of the pump, signal, and idler photons calculated by the Sellmeier equation.[41] Due to the law of energy conservation, the angle of PEA is always fixed at 135°. The angle of PMA is determined by the group velocity matching (GVM) condition, and the group velocity is μ_j, namely,

$$\mu_j = 1/k_j' = \mathrm{d}\Omega_j/\mathrm{d}k_j, \quad (6)$$

where Ω_j ($j = \mathrm{p,s,i}$) is the central frequency of the pump, signal, and idler photons. The angle for the pinch of PMA can be written as

$$\theta = -\arctan\frac{\mu_\mathrm{p}^{-1} - \mu_\mathrm{s}^{-1}}{\mu_\mathrm{p}^{-1} - \mu_\mathrm{i}^{-1}}. \quad (7)$$

For getting the spectrally uncorrelated biphoton state, there are three types of GVM conditions: $\theta = 0°$, 45°, and 90°, respectively.

Normally, the degree of spectral factorability can be calculated by performing Schmidt decomposition[43,44] on the JSA. It is written as a product of two orthogonal basis vectors $\phi_n(\omega_\mathrm{s})$ and $\varphi_n(\omega_\mathrm{i})$ as

$$f(\omega_\mathrm{s},\omega_\mathrm{i}) = \sum_n c_n \phi_n(\omega_\mathrm{s})\varphi_n(\omega_\mathrm{i}), \quad \sum_n c_n^2 = 1. \quad (8)$$

The Schmidt number K is calculated by $K = 1/\sum_n c_n^4$. And the spectral-purity P is equal to the inverse of K,

$$P = \frac{1}{K} = \sum_n c_n^4. \quad (9)$$

For a pure biphoton state, the Schmidt number $K = 1$ ($P = 1/K = 1$) which means a perfect factorable state is achieved, and thus the JSA is separable: $f(\omega_\mathrm{s},\omega_\mathrm{i}) = \phi_j(\omega_\mathrm{s})\varphi_j(\omega_\mathrm{i})$

2.1. Numerical simulation

Focus on the non-degenerate type-I SPDC process in the MgO:PPLN crystal with a poling period of 20.35 μm. When the temperature is below 35 °C, we find that the angle of PMA's contour could be 45° which means the contour of JSA is a circle, the non-degenerate telecom wavelength can be tuned mainly by changing the temperature. However, when the temperature is above 35 °C and the angle of PMA's contour is 90° which means the contour of JSA is an ellipse, the non-degenerate MIR wavelength can be achieved mainly by changing the pump wavelength. By changing the temperature and pump wavelength, the non-degenerate wavelengths will be continuously tuned from 1644.0 nm to 4922.9 nm which occupy a large part of the transparency window of LN, as shown in Fig. 1.

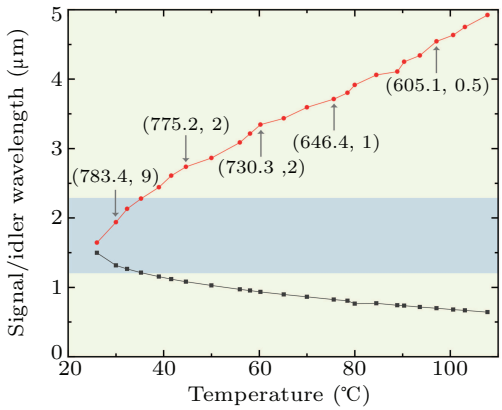

Fig. 1. Numerical calculations of signal and idler wavelengths versus temperature for high spectral-purity at non-degenerate type-I SPDC process in MgO:PPLN. For each temperature on the x-axis, the pump wavelength can obtained by the law of energy conservation and the pump bandwidth should be selected properly to maximize the spectral-purity which is above 0.74 in the whole wavelength range (1644.0 nm–4922.9 nm). In the light blue area, the temperature is below 35 °C, the pump wavelength is fixed at 783.4 nm and the non-degenerate wavelength can be finely tuned with temperature control. In the light green area, the temperature is above 35 °C and the non-degenerate wavelength can be finely tuned with temperature or pump wavelength control. Besides these, we list the pump wavelength and bandwidth conditions with a nanometer unit for high spectral-purity heralded single photons at some specific points.

The crystal length L and the poling period are fixed at 25 mm and 20.35 μm, respectively. For simplicity, we choose some specific temperatures, and the details of numerical simulation results are listed in Table 1. The symbols T, λ_p, and λ_i represent the sample temperature, wavelengths of pump and idler photons, and $\Delta\lambda_p$ represents the bandwidth of the pump laser. The symbol P_1 represents the purity of the photon pairs without any filters. The symbol η represents the filter efficiency when we apply a wide-band filter based on a Gaussian distribution on the signal photons for improving the purity to 0.95 which is represented by the symbol P_2.

To further demonstrate the spectral correlation conditions graphically, the simulating contours of JSA are shown in Fig. 2. When the sample temperature is set at 26 °C and 30 °C, the angle of PMA's contour $\theta = 45°$. Under the temperature of 50 °C, 70 °C, 80 °C, and 107.8 °C, the angle of PMA's contour $\theta = 90°$.

Table 1. Results of numerical calculations at some specific temperatures and pump wavelengths.

T (°C)	λ_p (nm)	$\Delta\lambda_p$ (nm)	λ_i (nm)	P_1	P_2	η (%)
26	783.4	9	1644.0	0.74	0.95	80.0
30	783.4	2	1938.2	0.86	0.95	91.7
50	755.4	2	2863.9	0.92	0.95	97.6
70	695.5	2	3593.1	0.86	0.95	84.8
80	661.9	1	3917.1	0.89	0.95	94.0
107.8	569	0.5	4922.9	0.88	0.95	92.6

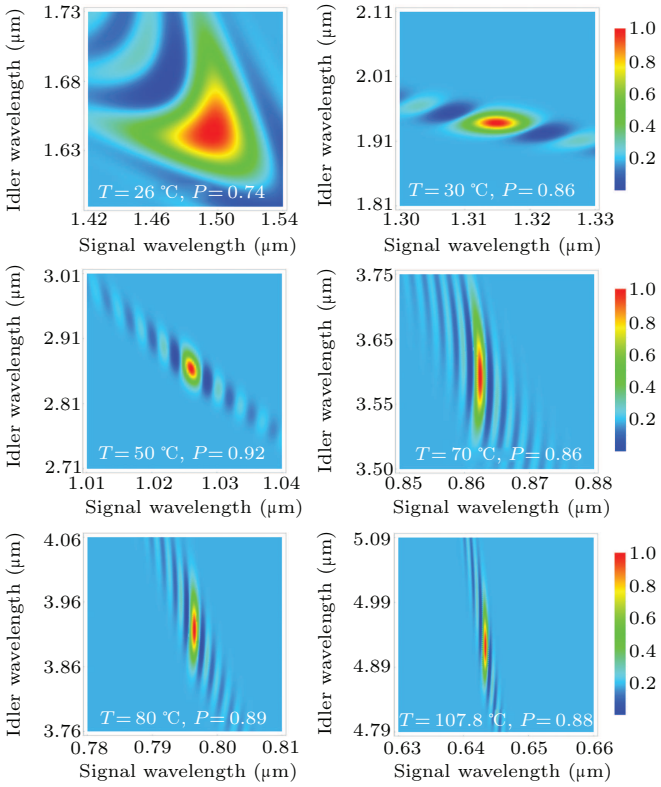

Fig. 2. The simulating contours of JSA in MgO:PPLN. The crystal length L and the poling period are fixed at 25 mm and 20.35 μm. The details of wavelengths are listed in Table 1. Respectively, by performing Schmidt decomposition on the JSA, the corresponding purities of photon pairs are 0.74, 0.86, 0.92, 0.86, 0.89, and 0.88 without any filters.

3. JSI and $g^{(2)}(0)$ measurement

3.1. JSI measurement and results

The experimental setup is shown in Fig. 3. The crystal (CTL PHOTONICS Ltd.) is periodically poled with a poling period of 20.35 μm for type-I SPDC. According to the simulation results, the temperature is fixed at 26 °C, the non-degenerate SPDC progress will be satisfied, $V_p(783.4\ \text{nm}) \rightarrow H_s(1496.6\ \text{nm}) + H_i(1644.0\ \text{nm})$, where the symbols p, s, and i represent the pump, signal, and idler photons, and H (V) represents the horizontal (vertical) polarization. Pump pulses from a mode-locded titanium sapphire laser are used to pump a 25 mm long MgO:PPLN crystal, the temporal duration ∼ 100 fs and repetition rate ∼ 79.49 MHz.

Traditional method of reconstructing the frequency correlation between the signal and idler photons is dependent on long dispersion compensating fibers (DCFs), which can make the different wavelengths mapping to different arrival times at the detector. This method is time consuming and has a low resolution. In our experiment, we choose a method named as "stimulated emission tomography"[20,42] to map the joint spectral intensity (JSI), which is faster and has a higher spectral resolution. For the JSI measurement, a tunable continuous wave (CW) laser (Santec-710) with a linewidth of 100 kHz is used as a seed light to simulate the emission of idler photons. The seed light is combined with the pump pulses by a PBS, and a $f = 15$ mm lens is used to focus the beams on the center of the crystal. The seed light and pump pulses propagate in the crystal collinearlly, and then the corresponding idler spectral mode in the JSI is amplified. A long-pass filter (FELH-1200; 1200 nm edge) is used to filter the pump laser. Another long-pass filter (FELH-1550; 1550 nm edge) is used to separate the seed light as a dichroic mirror (DM). The amplified spectra is collected into a single mode fiber through port a and routed to the optical spectrum analyzer (OSA) with a spectral accuracy of 0.065 nm.

The lasers used in the stimulated emission progress have an average power of up to 1.1 W and 3 mW for the pump and seed light, respectively. The power of the amplified spectra is high enough to be detected by the OSA and the wavelength is also recorded. A computer is used to control the wavelength of the CW laser and record the optical spectrum which is detected by the OSA. The wavelength of the seed light scans from 1450 nm to 1525 nm with a step of 0.1 nm. The numerical and experimental results which show a good agreement are present in Figs. 4(a) and 4(b), respectively. To further evaluate the spectral uncorrelation, we perform the Schmidt decomposition[43,44] on the JSI, from which we can estimate the single-photon purity to be 0.93. Due to the lost of phase information in the JSI, the spectral-purity estimated from the JSI is the upper limit.

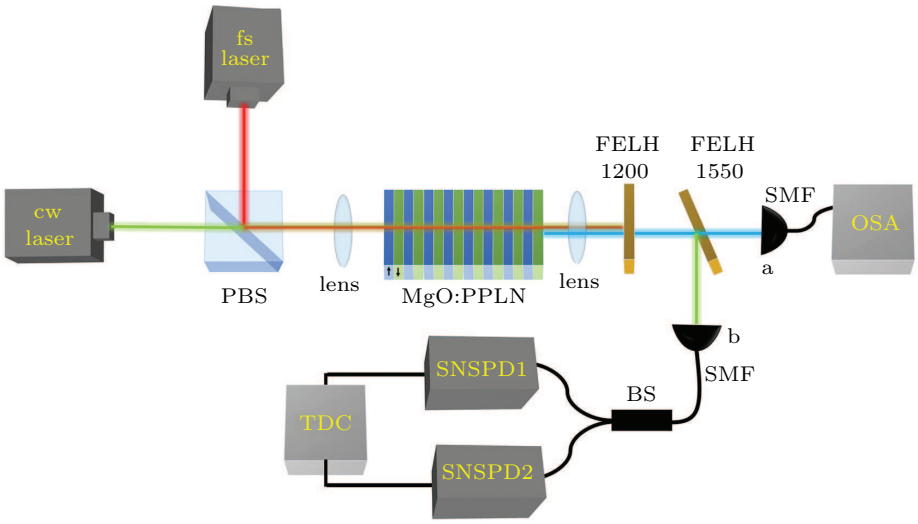

Fig. 3. The experimental setup. PBS: polarization beam splitter, FELH-1200: long-pass filter, FELH-1550: long-pass filter, OSA: optical spectrum analyzer, SMF: single mode fiber, SNSPD: superconducting nanowire single photon detector, TDC: time-to-digital converter. For the JSI measurement, a continuous-wave (cw) laser (Santec-710) is used as the signal seed injected together with the fs laser. The idler light is coupled into OSA by port a to measure the spectrum against the wavelength of the cw laser. For the $g^{(2)}(0)$ measurement, we turn off the cw laser. The generated signal photons are coupled into the BS by port b, and the photons are routed to SNSPD 1 and SNSPD 2, with the coincidence counts given by TDC.

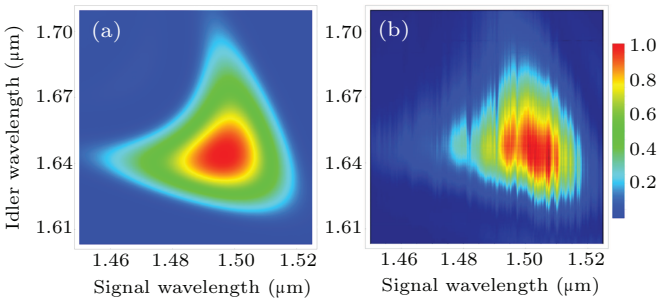

Fig. 4. (a) Numerical simulation of the JSI. The pump wavelength $\lambda_p = 783.4$ nm, the bandwidth of pump laser $\Delta\lambda_p = 9$ nm, the crystal length $L = 25$ mm, the temperature is 26 °C. (b) Experimental measured JSI. The experimental configuration is same as the numerical simulation.

3.2. The $g^{(2)}(0)$ measurement and results

Although the stimulated emission tomography graphically reveals the JSI with very high precision. However, the JSI measurement process is a phase-insensitive process. In experiment, the Glauber's second-order self-correlation function $g^{(2)}(0)$[45] is another important and direct method to quantify the purity of photons, and the purity is obtained by $P = g^{(2)}(0) - 1$.

The experimental setup is shown in Fig. 3 and the configuration is same as the JSI measurement process. For a $g^{(2)}(0)$ measurement, we turn off the tunable CW laser and reduce the average power of the pump to 6.3 mW. The down-conversion signal photons are collected into a single mode fiber through port b. The photons are split by a fiber 50 : 50 beam splitter (BS) then detected by two superconducting nanowire single photon detectors (SNSPD), and a time-to-digital converter (TDC) is used for the two-photon coincidence measurement. The detection efficiencies of SNSPD 1 and SNSPD 2 at wavelength 1496.6 nm are 76% and 65%, respectively. Two SNSPDs' single count rates and coincidence count rate are recorded as R_1, R_2, and R_{cc}, respectively. Then the $g^{(2)}(0)$ is calculated by

$$g^{(2)}(0) = \frac{R_{cc}R}{R_1 R_2}, \tag{10}$$

where $R = 79.49$ MHz is the pump repetition rate. By subtracting the dark counts, single count rates are 69890 Hz and 50080 Hz for R_1 and R_2, respectively. The coincidence counting rate $R_{cc} = 75.7$ Hz. Thus, $g^{(2)}(0) = 1.72 \pm 0.01$, corresponding to the purity $P = 0.72 \pm 0.01$, which agrees well with this estimated from the JSA in Fig. 2. Based on the numerical calculations in Table 1, we can estimate that the spectral-purity can be improved to 0.95 with 80.0% transmission efficiency. Due to the lack of the EPM conditions in type-0 and type-II SPDC processes, for getting the same non-degenerate wavelengths at the temperature of 26 °C, the spectral-purity estimated from the JSA is 0.10 and 0.24. The purity should be improved to 0.95, Gaussian filters much narrower than the photon bandwidths are employed, and the transmission efficiencies are 1.2% and 16.1%, respectively. Obviously, compared with the 80.0% transmission efficiency, the EPM method is an important and efficient way to get the single photons with high spectral-purity.

4. Conclusion

In this paper, by using a type-I, non-degenerate SPDC process in a single MgO:PPLN with fixed poling period and crystal length, we have generated a single-photon source with a high purity over a broad bandwidth. By changing the temperature and pump wavelength, we can get a widely tunable wavelength from 1644 nm to 4922.9 nm. The purity can be improved to 0.95 by a wide-band Gaussian filter, and the probability of signal photons passing the filter is above 0.8. Due

to wavelength limitation in the tunable CW laser, we only carry out the JSI and $g^{(2)}(0)$ measurements at a temperature of 26 °C. The JSI is obtained by the method of stimulated emission tomography with high precession. These experiment results are well consistent with the numerical simulations. We hope our widely tunable single photon source can play an important role in the future quantum technologies.

References

[1] Daniel G and Isaac L C 1999 *Nature* **402** 390
[2] Knill E, Laflamme R and Milburn G J 2001 *Nature* **409** 46
[3] Alberto P, Jonathan C F M and Jeremy L O B 2009 *Science* **325** 1221
[4] Jacob M, Nicholas C H, Gregory R S, Yoav L and Dirk E 2015 *Phys. Rev. A* **92** 032322
[5] Matthew A B, Alessandro F, Saleh R K, Justin D, Scott A, Timothy C R and Andrew G W 2013 *Science* **339** 794
[6] Andrea C, Roberto O, Roberta R, Daniel J B, Ernesto F G, Nicolò S, Chiara V, Enrico M, Paolo Mataloni and Fabio S 2013 *Nat. Photon.* **7** 545
[7] Max T, Borivoje D, René H, Stefan N, Alexander S and Philip W 2013 *Nat. Photon.* **7** 540
[8] Zhong H S, Wang H, Deng Y H, Chen M C, Peng L C, Luo Y H, Qin J, Wu D, Ding X, Hu Y, Hu P, Yang X Y, Zhang W J, Li Y X, Jiang X, Gan L, Yang G W, You L X, Wang Z, Li L, Liu N L, Lu C Y, Pan J W 2020 *Science* **370** 1460
[9] Nicolas S, Christoph S, Hugues R and Nicolas G 2011 *Rev. Mod. Phys.* **83** 33
[10] Koji A, Kiyoshi T and Hoi K L 2015 *Nat. Commun.* **6** 6787
[11] Temporao G, Zbinden H, Tanzilli Jean S, Gisin N, Aellen T, Giovannini M E, Faist J and Von Der Weid J P 2008 *Quantum Inf. Comput.* **8** 1
[12] Fernandez D C, Bhargava R, Hewitt S M and Levin I W 2005 *Nat. Biotechnol.* **23** 469
[13] Amrania H, Antonacci G, Chan C H, Drummond L, Otto W R, Wright N A and Phillips C 2012 *Opt. Express* **20** 7290
[14] Raghi S E, Diaa K and Mohamed A S 2020 *Sci. Rep.* **10** 1293
[15] H∅gstedt L, Dam J S, Sahlberg A L, Li Z S, Aldén M, Pedersen C and Lichtenberg P T 2014 *Opt. Lett.* **39** 5321
[16] Lee K J, Lee S and Shin H 2016 *Appl. Opt.* **55** 9791
[17] Bellei F, Cartwright A P, McCaughan A N, Dane A E, Najafi F, Zhao Q Y and Berggren K K 2016 *Opt. Express* **24** 3248
[18] Tan S H, Erkmen B I, Giovannetti V, Guha S, Lloyd S, Maccone L, Pirandola S and Shapiro J H 2008 *Phys. Rev. Lett.* **101** 253601
[19] Wang Q, Hao L, Zhang Y, Xu L, Yang C, Yang X and Zhao Y 2016 *Opt. Express* **24** 5045
[20] Liu Y W, Wu C, Gu X W, Kong Y C, Yu X X, Ge R Y, Cai X L, Qiang X G, Wu J J, Yang X J and Xu P 2020 *Opt. Lett.* **45** 73
[21] Zhu P Y, Liu Y W, Wu C, Xue S C, Yu X Y, Zheng Q L, Wang Y, Qiang X G, Wu J J and Xu P 2020 *Chin. Phys. B* **29** 114201
[22] Chen C C, Bo C, Niu M Y, Xu F H, Zhang Z S, Jeffrey H S and Franco N C W 2020 *Opt. Express* **25** 7300
[23] Jin R B, Ryosuke S, Kentaro W, Hugo B and Masahide S 2013 *Opt. Express* **21** 10659
[24] Kaneda F, Palmett K G, U'Ren A B and Kwiat P G 2016 *Opt. Express* **24** 10733
[25] Liu Y C, Guo D J, Ren K Q, Yang R, Shang M H, Zhou W, Li X H, Sun C W, Xu P, Xie Z D, Gon Y X and Zhu S N 2021 *Sci. Rep.* **11** 12628
[26] Wang J, Zhang C H, Yang L J, Qian X R, Li J and Wang Q 2021 *Chin. Phys. B* **30** 070304
[27] Sun C W, Wu S H, Duan J C, Zhou J W, Xia J L, Xu P, Xie Z D, Gong Y X and Zhu S N 2019 *Opt. Lett.* **44** 5598
[28] Ma B, Wei S H, Chen Z S, Shang X J, Ni H Q and Niu Z C 2018 *Chin. Phys. B* **27** 097802
[29] Zhang Q Y, Xu P and Zhu S N 2018 *Chin. Phys. B* **27** 054207
[30] Gisin N, Ribordy G, Tittel W and Zbinden H 2002 *Rev. Mod. Phys.* **74** 145
[31] Upton L, Harpham M, Suzer O, Richter M, Mukamel S and Goodson T 2013 *J. Phys. Chem.* **4** 2046
[32] Bránczyk A M, Ralph T C, Helwig W and Silberhorn C 2010 *New J. Phys.* **12** 063001
[33] Christ A, Lupo C, Reichelt M, Meier T and Silberhorn C 2014 *Phys. Rev. A* **90** 023823
[34] Evan M S, Nicola M, Johannes T, Linda S, Harald H, Tim J B and Christine S 2017 *Phys. Rev. A* **95** 061803
[35] Vittorio G, Lorenzo M, Jeffrey H S and Franco N C W 2002 *Phys. Rev. Lett.* **88** 183602
[36] Vittorio G, Lorenzo M, Jeffrey H So and Franco N C W 2002 *Phys. Rev. A* **66** 043813
[37] Zhang Q Y, Xue G T, Xu P, Gong Y X, Xie Z D and Zhu S N 2018 *Phys. Rev. A* **97** 022327
[38] Jin R B, Cai N, Huang Y, Hao X Y, Wang S, Li F, Song H Z, Zhou Q and Shimizu R 2019 *Phys. Rev. A* **11** 034067
[39] Laudenbach F, Jin R B, Greganti C, Hentschel M,Walther P and Hübel 2017 *Phys. Rev. Appl.* **8** 024035
[40] Wei B, Cai W H, Ding C L, D G W, Shimizu R, Zhou Q and Jin R B 2021 *Opt. Express* **29** 256
[41] Gayer O, Sacks Z, Galun E and Arie A 2008 *Appl. Phys. B* **91** 343
[42] Liscidini M and Sipe J E 2013 *Phys. Rev. Lett.* **111** 193602
[43] Law C K, Walmsley I A and Eberly J H 2000 *Phys. Rev. Lett.* **84** 5304
[44] Fabian L, Hannes H, Michael H, Philip W and Andreas P 2016 *Opt. Express* **24** 2712
[45] Andreas C, Kaisa L, Andreas E, Katiúscia N C and Christine S 2011 *New J. Phys.* **13** 033027